

Gait Speed Estimation from Millimeter-Wave Wireless Sensing

Zhuangzhuang Gu; Hem Regmi; Sanjib Sur Computer Science and Engineering; University of South Carolina, Columbia, USA zg5@email.sc.edu; hregmi@email.sc.edu; sur@cse.sc.edu

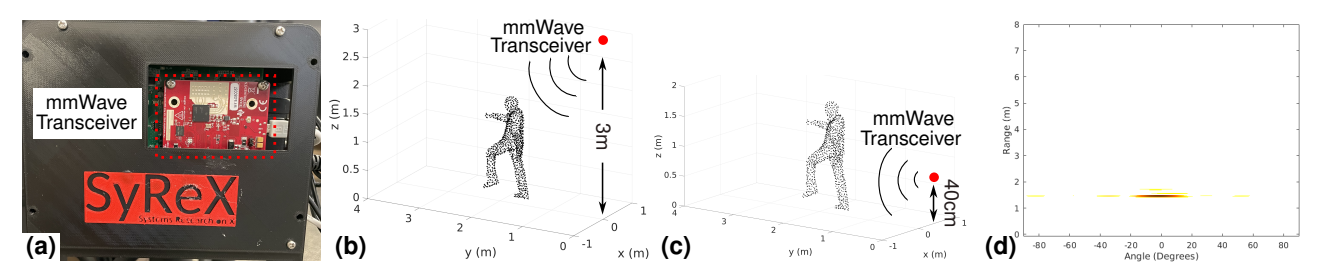


Figure 1: (a) Millimeter-wave transceiver; (b) Mounting device near to ceiling; (c) Mounting device near to ground; (d) A snapshot of Dynamic Range-Angle heatmap from ground device.

ABSTRACT

Gait speed is an important indicator of human health. Monitoring patients' gait speed can help doctors assess the recovery process, but traditional clinician observation fails to track in home scenarios. Compared to vision-based and wearable approaches, radio frequency signals offer an easily deployable and light free solution protecting user privacy in home scenarios. Therefore, we proposed a millimeter-wave (mmWave) system to accurately extract walking periods from collected trials and calculate gait speeds. To evaluate the robustness and reliability of our system and determine the optimal mounting position, we collected data from 5 volunteers with normal walking speeds and imitated various abnormal gait patterns and walking speeds. The results show that the mmWave device mounted near the ground outperforms across all volunteers than the one mounted near the ceiling, achieving an average estimation error of 0.02 m/s in abnormal gait evaluations.

CCS CONCEPTS

Hardware → Sensor applications and deployments.



This work is licensed under a Creative Commons Attribution International 4.0 License. MobiCom'24, Nov. 18-22, 2024, Washington, D.C., USA © 2024 Copyright held by the owner/author(s). https://doi.org/10.1145/3636534.3697439

KEYWORDS

Millimeter-wave; Deep Learning; Gait Speed Measurement

ACM Reference Format:

Zhuangzhuang Gu; Hem Regmi; Sanjib Sur, Computer Science and Engineering; University of South Carolina, Columbia, USA, zg5@email.sc.edu; hregmi@email.sc.edu; sur@cse.sc.edu . 2024. Gait Speed Estimation from Millimeter-Wave Wireless Sensing. In MobiCom'24: The 30th Annual International Conference on Mobile Computing and Networking, Nov. 18-22, 2024, Washington, D.C., USA. ACM, New York, NY, USA, 3 pages.

1 INTRODUCTION

Human gait refers to the pattern of walking involving the center movement of gravity during locomotion [1]. Since the gait pattern is often compromised by various musculoskeletal and neurological conditions or diseases, such as stroke, it can reflect levels of independence, quality of life and participation [5]. Gait speed, in particular, is validated as a key indicator of health, enabling clinicians to easily assess the cognitive states of patients [3, 4]. A change in walking speed of 0.05 m/s is clinically considered a meaningful improvement [3], which helps doctors evaluate the recovery process of patients.

Traditional gait speed measurement relies heavily on clinician observation, requiring patients to walk a specified distance while timing them with a stopwatch [4]. This method needs time-consuming medical visits and cannot monitor patients' health status at home. Wearable sensors combining accelerometer, gyroscope, and GPS have been used to monitor walking speed, but these devices mostly make patients, especially older adults, feel uncomfortable. RGB-D camera can provide detailed 3D point clouds and RGB images to

capture human gait, but the privacy concern and lighting requirement significantly limit its application at home [2].

Millimeter-wave signals, with their distinctive features such as high resolution, light-free operation, low-cost, and no privacy invasion, have attracted researchers to track and analyze human activities. Therefore, we propose this gait speed estimation system based on mmWave reflections, which can accurately generate human body location from range-angle heatmaps (RAMaps), separate walking periods from continuous activities for measurement, and finally calculate the gait speed. Our system doesn't require any wearable sensors on the user's body and can function well in low-light conditions. Compared to vision-based works, the privacy-protecting characteristics of our system allow it to be applied in various home environments, such as bedrooms.

To determine the optimal mounting position for the mmWave device, we tested two setups: one near the ceiling and one close to the ground (Fig. 1[a-c]). To evaluate this system, we collected data from 5 volunteers with normal walking speed for both setups. Additionally, we imitated the abnormal gait patterns of patients at different walking speeds to analyze the performance of our work. The ground-mounted device estimated gait speed more accurately than the top-mounted setup across all volunteers. Furthermore, the ground-mounted device can conveniently access power from wall outlets, facilitating the deployment of this system. The average estimation error of 0.02 m/s in various abnormal gait patterns highlights the robustness and reliability of our system.

2 SYSTEM DESIGN

To accurately estimate the gait speed, our system is mainly consist of two components: *Generating Body Location* and *Separating Walking Periods*.

2.1 Generating Body Location

To effectively generate body locations from raw mmWave reflections, we first produce dynamic RAMaps (Fig. 1[d]) to extract moving targets from static surrounding objects. The dynamic RAMaps generation involves 3 steps: Range FFT transforming the time domain signals into the frequency domain, Dopple FFT applied on continuous frames to differentiate the moving subjects from stationary surroundings, and Angle FFT calculating the azimuth angle from non-overlapping virtual antennas. From the visualized dynamic RAMaps, continuous body movement can be captured by detecting the large connected regions and converting the range and angle values into accurate 2D locations in bird's eye view (BEV). To filter out noise points in the dynamic RAMaps, we threshold the moving distances of multiple detected targets between two continuous frames, accounting for the limited walking speeds. In non-moving periods, the dynamic RAMaps cannot detect

anything, and the generated body location remains the same as the last detected one.

2.2 Separating Walking Periods

To correctly identify the walking segments, we first utilize a sliding window with long time duration to monitor body location changes. The transitions from small location vibrations to large body movements indicate the start of a walking period. Then, we slice the long time window into shorter time windows to find the precise start frame of walking. A similar method is applied to detect the exact end frames of walking segments. However, the reflected mmWave signals from different parts of human body cause variations of generated body locations, since the mmWave device provides very limited angle information in the vertical plane. The detected targets in the same position will generate different body locations due to the lack of height information. These variations of body locations challenge our system to determine the start and end frames of walking periods. Therefore, we design a smoothing window to filter out those exceptional location changes. This smoothing window requires stable large motions over a specific time duration, which helps denoise the location variations from mmWave signals and improves the accuracy of walking segmentation. Eventually, we can calculate the gait speed from location changes and time duration for each walking segment.

3 PRELIMINARY RESULTS

Top-mounted mmWave transceivers can avoid ground obstacles to easily track human locations, but body reflections projected on the heatmap will amplify the detected spots to reduce accuracy, and focus shifts cause location vibrations, disrupting walking detection. Therefore, we implemented ground-mounted setup for accurate body location, providing easier power access than top-mounted. To evaluate our gait speed estimation system with two setups, we collected mmWave reflections from 5 volunteers with normal walking speeds and simulated abnormal walking patterns and speeds of patients. For each case, we captured multiple walking segments, also called trials, to evaluate our system. Fig. 2 and Fig. 3 display the scatter plot of predicted and ground-truth gait speeds from ground-mounted and top-mounted devices. A higher correlation coefficient indicates that the prediction is closer to the ground truth, with the green line showing where the predictions exactly match the ground-truth values. In general, the ground-mounted device, achieving correlation coefficient of 0.99, outperforms the top-mounted device. Particularly, when the walking speed is low, the top-mounted device fails to detect walking segments from human activity because inaccurate body locations heavily affect the threshold values used to distinguish walking from standing. To validate

the robustness of our ground-mounted system in handling abnormal gait, we simulated various walking patterns of the patients at different speeds around 0.2 m/s, 0.4 m/s, and 0.6 m/s (see Fig. 4). The low average error of estimated gait speed demonstrates our system, with ground-mounted device, is robust and reliable enough to handle abnormal gait. For example, in the case 6, walking in a straight line with angles at a speed of around 0.2 m/s, our ground-mounted device achieves an average error of 0.003 m/s, while top-mounted device cannot detect any walking segment. Fig. 5 demonstrates that the top-mounted device fails to correctly segment walking periods in various abnormal gait cases due to the vibrations of body locations.

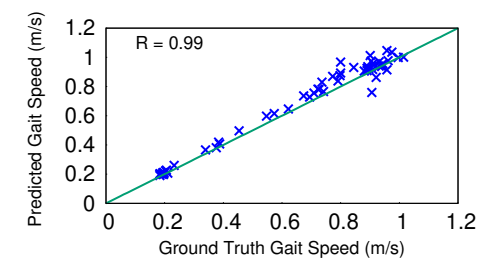


Figure 2: The scatter plot of the ground-mounted device across all trials is displayed. The green line indicates where the predictions exactly match the ground-truth values. The correlation coefficient (R) is 0.99.

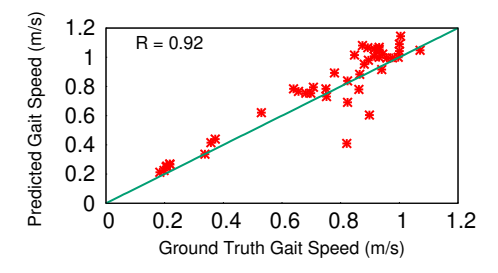


Figure 3: The scatter plot of top-mounted device across all trials. The correlation coefficient (R) is 0.92.

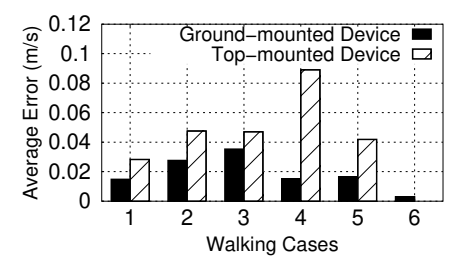


Figure 4: The performance of two setups on abnormal gait. Cases 1-3 demonstrate the simulated walking at speeds around 0.2 m/s, 0.4 m/s, and 0.6 m/s, respectively. Cases 4-6 depict walking at speed around 0.2m/s in different patterns: straight line, spiral path, and line path with different angles.

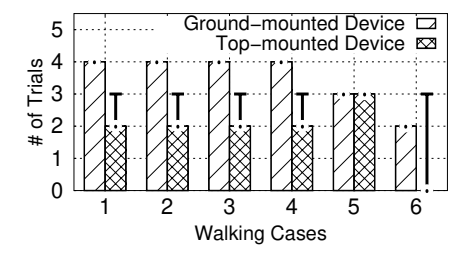


Figure 5: This figure shows the number of detected and missed walking trials for two setups. The shaded bars represent the number of detected walking trials, while the error bars display the missed trials compared to the ground truth.

4 CONCLUSION AND FUTURE WORKS

This work presents a gait speed estimation system utilizing mmWave reflections to generate precise body locations from dynamic RAMaps and estimate speeds from separated walking periods. We evaluated our system across 5 volunteers with normal walking speeds and validated its reliability and robustness on abnormal gait patterns at various speeds. The results demonstrate that the ground-mounted device excels in measuring gait speeds and achieves high accuracy even on abnormal gait. In the future, we plan to collect data from real stroke patients and extend our system to accurately predict the 3D feet locations of patients, which enables significant applications on patients, such as monitoring the recovery process and correcting exercise posture.

ACKNOWLEDGMENTS

This work is partially supported by the NSF under grants CAREER-2144505, NeTS-2342833, and MRI-2018966.

REFERENCES

- [1] Abdullah S Alharthi et al. 2019. Deep Learning for Monitoring of Human Gait: A Review. *IEEE Sensors Journal* 19, 21 (2019).
- [2] Amandine Dubois et al. 2014. A Gait Analysis Method Based on a Depth Camera for Fall Prevention. In 2014 36th Annual International Conference of the IEEE Engineering in Medicine and Biology Society.
- [3] Stacy Fritz et al. 2009. White Paper: "Walking Speed: the Sixth Vital Sign". *Journal of Geriatric Physical Therapy* 32, 2 (2009).
- [4] Chen-Yu Hsu et al. 2017. Extracting Gait Velocity and Stride Length from Surrounding Radio Signals. In Proceedings of the 2017 CHI Conference on Human Factors in Computing Systems.
- [5] Kara K Patterson et al. 2012. Gait Symmetry and Velocity Differ in Their Relationship to Age. Gait & Posture 35, 4 (2012).